Modeling Transition State Solvation at the Single-Molecule Level: Test of Correlated *ab Initio* Predictions against Experiment for the Gas-Phase S_N2 Reaction of Microhydrated Fluoride with Methyl Chloride

Wei-Ping Hu and Donald G. Truhlar*

Contribution from the Department of Chemistry and Supercomputer Institute, University of Minnesota, Minneapolis, Minnesota 55414-0431

Received December 9, 1993. Revised Manuscript Received May 31, 1994®

Abstract: Extended-basis-set calculations including electron correlation have been carried out on the reactants, products, and saddle point of the gas-phase S_N2 reaction $F^-(H_2O) + CH_3Cl$ and its deuterium substituted analogs. Transition state theory (TST) rate constants and secondary deuterium kinetic isotope effects (KIEs) are calculated for both CD_3 and D_2O substitution, and the results are in excellent agreement with recent experiments.

1. Introduction

Gas-phase S_N2 reactions[1] continue to be the target of experimental[2] and theoretical[3] studies because these reactions provide the prototype of the ubiquitous displacement mechanism. Recent experimental advances have opened the door to detailed study of S_N2 reactions of gas-phase microsolvated clusters,[4,5] which is a previously missing link between vapor-phase and solution kinetics. In this paper, stimulated by recent experiments of O'Hair *et al.*[5] we report a theoretical study of the reactions

$$F^-(H_2O) + CH_3Cl \rightarrow Cl^- + CH_3F + H_2O \qquad (R1a)$$

$$\rightarrow Cl^-(H_2O) + CH_3F \qquad (R1b)$$

and of the three analogous reactions in which the two hydrogen atoms in the water and/or the three hydrogen atoms in the methyl chloride are replaced by deuterium. We performed electronic structure calculations to optimize the geometrices and to calculate the energies and harmonic vibrational frequencies of the reactants, products, and the saddle points of these reactions. We then used this information to calculate transition state theory[6] rate constants and the secondary kinetic isotope effects (KIEs). Since our previous experience[3e,h,l,m] with similar S_N2 reactions in the gas phase indicated that variational optimization of the transition state location and the inclusion of tunneling effects[3l] have only minor or negligible effects on the reaction rates and kinetic isotope effects (KIEs), we will limit ourselves to conventional transition state theory in this paper. The question of whether dynamic recrossing effects[7] contribute to the breakdown of the fundamental assumption of transition state theory is still open,[3f,g,k-m] and tests such as the present ones, where conventional transition state theory is compared quantitatively to experiment, provide the essential data needed to complete that story.

2. Computational Methods

The basis sets we used in the electronic structure calculations are Dunning's[8] augmented correlation consistent polarized valence double-ζ (aug-cc-pVDZ) and augmented correlation consistent polarized valence triple-ζ (aug-cc-pVTZ) basis sets. The aug-cc-pVDZ set was used for geometry optimization and energy and frequency calculations on reactants, products, and transition states, while the aug-cc-pVTZ was only used for geometry optimization and energy calculations for the reactants and products. All the calculations involve geometries optimized while including electron correlation at the Møller–Plesset[9] second-order many-body [typically abbreviated MP2[10a] or D-MBPT(2)[10b]] or higher[11] level.

Full details of calculated geometries, total energies, and vibrational frequencies are given in the supplementary material.

* Abstract published in *Advance ACS Abstracts,* July 15, 1994.

(1) Reviews have been given by the following: (a) Riveros, J. M.; Jose, S. M.; Takashima, I. *Adv. Phys. Org. Chem.* **1985**, *21*, 197. (b) Shaik, S. S.; Schlegel, H. B.; Wolfe, S. *Theoretical Aspects of Physical Organic Chemistry: The S_N2 Mechanism*; John Wiley & Sons: New York, 1992.

(2) (a) Su, T.; Morris, R. A.; Viggiano, A. A.; Paulson, J. F. *J. Phys. Chem.* **1990**, *94*, 8426. (b) Gronert, S.; DePuy, C. H.; Bierbaum, V. M. *J. Am. Chem. Soc.* **1991**, *113*, 4009. (c) Viggiano, A. A.; Paschkewitz, J. S.; Morris, R. A.; Paulson, J. F.; Gonzalez-Lafont, A.; Truhlar, D. G. *J. Am. Chem. Soc.* **1991**, *113*, 9404. (d) Graul, S. T.; Bowers, M. T. *J. Am. Chem. Soc.* **1991**, *113*, 9696. (e) Cyr, D. M.; Posey, L. A.; Bishea, G. A.; Han, C.-C.; Johnson, M. A. *J. Am. Chem. Soc.* **1991**, *113*, 9697. (f) Wilbur, J. L.; Brauman, J. I. *J. Am. Chem. Soc.* **1991**, *113*, 9699. (g) Wladkowski, B. D.; Lim, K. f.; Allen, W. D.; Brauman, J. I. *J. Am. Chem. Soc.* **1992**, *114*, 9136. (h) Viggiano, A. A.; Morris, R. A.; Paschkewitz, J. S.; Paulson, J. F. *J. Am. Chem. Soc.* **1992**, *114*, 10477.

(3) For theoretical work not in ref 1b, see: (a) Morokuma, K. *J. Am. Soc. Chem.* **1982**, *104*, 3732. (b) Ohta, K.; Morokuma, K. *J. Phys. Chem.* **1985**, *89*, 5845. (c) Evanseck, J. D.; Blake, J. F.; Jorgensen, W. L. *J. Am. Chem. Soc.* **1987**, *109*, 2349. (d) Hirao, K.; Kebarle, P. *Can. J. Chem.* **1989**, *67*, 1261. (e) Tucker, S. C.; Truhlar, D. G. *J. Am. Chem. Soc.* **1990**, *94*, 3338, 3347. (f) Vande Linde, S. R.; Hase, W. L. *J. Phys. Chem.* **1990**, *94*, 6148. (g) Vande Linde, S. R.; Hase, W. L. *J. Chem. Phys.* **1990**, *93*, 7962. (h) Zhao, X. G.; Tucker, S. C.; Truhlar, D. G. *J. Am. Chem. Soc.* **1991**, *113*, 826. (i) Gonzalez-Lafont, A.; Truong, T. N.; Truhlar, D. G. *J. Phys. Chem.* **1991**, *95*, 4618. (j) Wolfe, S.; Kim, C.-K. *J. Am. Chem. Soc.* **1991**, *113*, 8056. (k) Cho, Y. J.; Vinde Linde, S. R.; Hase, W. L. *J. Chem. Phys.* **1992**, *96*, 8275. (l) Zhao, X. G.; Lu, D.-h.; Liu, Y.-P.; Lynch, G. C.; Truhlar, D. G. *J. Chem. Phys.* **1992**, *97*, 6369. (m) Truhlar, D. G.; Lu, D.-h.; Tucker, S. C.; Zhao, X. G.; Gonzalez-Lafont, A.; Truong, T. N.; Maurice, D.; Liu, Y.-P.; Lunch, G. C. *ACS Symp. Ser.* **1992**, *502*, 16. (n) Barnes, J. A.; Williams, I. H. *J. Chem. Soc., Chem. Commun.* **1993**, 1286.

(4) (a) Bohme, D. K.; Raksit, A. B. *Can. J. Chem.* **1984**, *106*, 3447. (b) Bohme, D. K.; Raksit, A. B. *Can. J. Chem.* **1985**, *63*, 3007. (c) Henchman, M.; Hierl, P. M.; Paulson, J. F. *J. Am. Chem. Soc.* **1985**, *107*, 2812. (d) Hierl, P. M.; Ahrens, A. F.; Henchman, M.; Viggiano, A. A.; Paulson, J. F.; Clary, D. C. *J. Am. Chem. Soc.* **1986**, *108*, 3142.

(5) O'Hair, R. A. J.; Dang, T. T.; DePuy, C. H.; Bierbaum, V. M. *J. Am. Chem. Soc.* submitted for publication.

(6) (a) Eyring, H. *J. Chem. Phys.* **1935**, *3*, 107. (b) Wigner, E. *Trans. Faraday Soc.* **1938**, *34*, 29.

(7) (a) Truhlar, D. G.; Garrett, B. C. *Acc. Chem. Res.* **1980**, *13*, 440. (b) Truhlar, D. G.; Isaacson, A. D.; Garrett, B. C. In *Theory of Chemical Reaction Dynamics*; Baer, M., Ed.; CRC Press; Boca Raton, FL, 1985; Vol. 4, p 65.

(8) (a) Dunning, T. H., Jr. *J. Chem. Phys.* **1989**, *90*, 1007. (b) Woon, D. E.; Dunning, T. H., Jr. *J. Chem. Phys.* **1993**, *98*, 1358.

(9) Møller, C.; Plesset, M. S. *Phys. Rev.* **1934**, *46*, 618.

(10) (a) Hehre, W. J.; Radom, L.; Schleyer, P. v. R.; Pople, J. A. *Ab initio Molecular Orbital Theory*; Wiley: New York, 1986. (b) Adams, G. F.; Bent, G. D.; Bartlett, R. J.; Purvis, G. D. In *Potential Energy Surfaces and Dynamics Calculations*; Truhlar, D. G., Ed.; Plenum: New York, 1981; p 133.

(11) Pople, J. A.; Head-Gordon, M. J. *J. Chem. Phys.* **1987**, *87*, 5968.

(12) Chase, M. W., Jr.; Davies, C. A.; Downey, J. R., Jr.; Frurip, D. J.; McDonald, R. A.; Syverud, A. N. *J. Phys. Chem. Ref. Data* **1985**, *14*, Suppl. 1.

0002-7863/94/1516-7797$04.50/0 © 1994 American Chemical Society

Table 1. Energies (Born–Oppenheimer ΔE) of Reaction in kcal/mol

reaction	MP2/aug-cc-pVDZ	MP2/aug-cc-pVTZ	expt[a]
R2	−30.5	−29.6	−31.9[b]
R3	+26.8	+27.6	+23.5[c]
R4	−14.7	−15.4	−15.6[d]
R1a	−3.7	−2.0	−8.4
R1b	−18.4	−17.4	−24.0

[a] Computed from experimental ΔH°_0 or ΔH°_{298} from reference given, corrected to ΔE by using the harmonic zero point energy and, for ΔH°_{298}, the thermal translational-rotational-vibrational excitation energy. [b] Reference 12. [c] Reference 13. [d] Reference 14.

Table 2. Rate Constants (in 10^{-11} molecule cm^3 s^{-1}) and Kinetic Isotope Effects at 300 K

reaction	quantity	PM3	MP2/aug-cc-pVDZ	expt[a]
$F^-(H_2O) + CH_3Cl$	k_H	1.43×10^{-5}	2.43	1.49 ± 0.02
$F^-(D_2O) + CH_3Cl$	KIE[b]	0.78	0.65	0.65 ± 0.03
$F^-(H_2O) + CD_3Cl$	KIE	1.53	0.83	0.85 ± 0.04
$F^-(D_2O) + CD_3Cl$	KIE	1.19	0.54	0.56 ± 0.01

[a] From ref 5. [b] KIE in each row of this table is defined as the ratio of k_H to the rate constant of the reaction in that row. In all cases, rates are summed over dissociated and nondissociated products, e.g., $k_H = k(\text{R1a}) + k(\text{R1b})$.

3. Results and Discussion

Consider the following reactions

$$F^- + CH_3Cl \rightarrow CH_3F + Cl^- \quad \text{(R2)}$$

$$F^-(H_2O) \rightarrow F^- + H_2O \quad \text{(R3)}$$

$$Cl^- + H_2O \rightarrow Cl^-(H_2O) \quad \text{(R4)}$$

R1a and R1b can be thermodynamically viewed as R2 + R3 and R2 + R3 + R4, respectively. The calculated and experimental[12-14] energies (Born–Oppenheimer ΔE) of these reactions and the resultant reaction energies for R1a and R1b are shown in Table 1. The table shows that the theoretical energetics of R3 are in significant disagreement with experiment, leading to an even larger discrepancy in ΔE for R1. We also performed an energy calculation on R3 with the aug-cc-pVDZ basis set at the QCISD(T)[11] level, and the calculated dissociation energy is 27.0 kcal/mol, which is very close to the MP2 result of 27.6 kcal/mol. However, it is known that dissociation and association energies are very difficult to calculate, especially those that involve fluorine. The discrepancy for R2 is in the direction expected when basis set superposition error[15] is important.

The calculated energy of the saddle point of R1 at the MP2/aug-cc-pVDZ level is −3.5 kcal/mol with respect to the reactants. Adding the zero point energy of the saddle point and subtracting that of reactants yields the vibrationally adiabatic ground-state barrier height, which is −2.2 kcal/mol. We used the information from the MP2/aug-cc-pVDZ calculations to perform transition state theory rate constant calculations at 300 K for the four isotopic versions of R1 listed in Table 2. The reaction is assumed to proceed as a binary collision as it does in the low-pressure limit. The calculations include all modes, and for vibrations they include both zero point and thermal vibrational effects. All the vibrational modes are treated harmonically. To test the validity of the harmonic approximation for the low-frequency modes we also employed the hindered rotor[16,17] treatment for the three lowest vibrational frequency modes of the transition state, and we found that the calculated rate constants with this more sophisticated treatment of vibrations differ from the harmonic values by less than 1%.

The calculated rate constants and KIEs for the perprotio and variously deuterium substituted reactions are shown in Table 2. Rate constants and KIEs calculated by the parameterized model 3[18] (PM3), a popular semiclassical method (which predicts a 5.3 kcal/mol classical barrier height), are also shown for comparison, as are the experimental results. In the MP2/aug-cc-pVDZ calculations, the calculated rate constants are a little too high; however if we adjust the classical barrier height to −3.22 kcal/mol (from the directly calculated value −3.51 kcal/mol), we can fit the experimental rate constant for the perprotio reaction exactly. Such a small change is well within the reliability of the calculated barrier height. The KIEs are independent of any adjustment in classical barrier height provided the harmonic force fields of the transition state and reactant are unchanged; such an adjustment would do nothing except lower all rate constants by the same factor. We note that the calculated KIEs from MP2/aug-cc-pVDZ calculations agree extremely well with experiments, in fact well within the stated experimental error bars. The poor agreement between the calculations based on PM3 and experiments is mainly because of the inaccuracy of the vibrational frequencies, and these results are provided merely to illustrate that the KIEs are indeed very sensitive to these frequencies (so that even a popular semiquantiative theoretical level is far from adequate).

Reaction to produce $Cl^-(H_2O) + CH_3F$ is exoergic by 24 kcal/mol, and reaction to produce $Cl^- + CH_3F + H_2O$ is exoergic by 8 kcal/mol. The experiments showed a branching ratio of 3:1 between R1a and R1b. However, in the calculated saddle point geometry the water molecule is still hydrogen bonded to the fluorine atom. Calculations in which we followed[19] the reaction path showed that the water molecule stays bound at the fluorine atom all the way down to the product ion–dipole complex. We failed to find another saddle point that corresponds to the reaction with the water molecule moving in a concerted way from the fluorine atom side to the chlorine atom side. Our calculations thus predict a nonsynchronous reaction path in which the H_2O molecule is transferred to the Cl^- after the dynamical bottleneck to reaction.

Further insight into the origin of the KIEs is provided by a factor analysis, as used previously for other reactions.[3h,i,l,m,20] The particular factorization

$$\text{KIE} = \eta_{\text{trans}}\,\eta_{\text{rot}}\,\eta_{\text{low}}\,\eta_{\text{mid}}\,\eta_{\text{high}} \quad (1)$$

where the factors, in the order they appear in eq 1, refer, respectively, to contributions from translational and rotational and from low-, mid-, and high-frequency vibrational modes has proved particularly informative in previous work,[3h,i,l,m] and these factors are given in Table 3. Using the standard notation by which KIEs and factors are "normal" when greater than 1 (with the lighter isotopic version always in the numerator) and "inverse" when less than 1, we see that the product of the vibrational factors is very inverse, being 0.46, 0.48, and 0.22 for the three reactions, respectively, but a large normal rotational factor brings the overall KIE closer to 1. Both low- and high-frequency modes contribute very significantly to the inverse KIE.

(13) Arshadi, M.; Yamdagni, R.; Kebarle, P. *J. Phys. Chem.* **1970**, *74*, 1475.
(14) Hiraoka, K.; Mizuse, S.; Yamabe, S. *J. Phys. Chem.* **1988**, *92*, 3943.
(15) Boys, S. F.; Bernardi, F. *Mol. Phys.* **1970**, *19*, 553.
(16) Truhlar, D. G. *J. Comput. Chem.* **1991**, *12*, 266.
(17) Lu, D.-h.; Truong, T. N.; Melissas, V. S.; Lynch, G. C.; Liu, Y.-P.; Garrett, B. C.; Steckler, R.; Isaacson, A. D.; Rai, S. N.; Hancock, G. C.; Lauderdale, J. G.; Joseph, T.; Truhlar, D. G. *Computer Physics Communications* **1992**, *71*, 235.
(18) Stewart, J. J. P. *J. Comput. Chem.* **1989**, *10*, 221.
(19) (a) Shavitt, I. *J. Chem. Phys.* **1968**, *49*, 4048. (b) Truhlar, D. G.; Kuppermann, A. *J. Am. Chem. Soc.* **1971**, *93*, 1840.
(20) (a) Garrett, B. C.; Truhlar, D. G.; Magnuson, A. W. *J. Chem. Phys.* **1982**, *76*, 2321. (b) Tucker, S. C.; Truhlar, D. G.; Garrett, B. C.; Isaacson, A. D. *J. Chem. Phys.* **1985**, *82*, 4102. (c) Lu, D.-h.; Maurice, D.; Truhlar, D. G. *J. Am. Chem. Soc.* **1990**, *112*, 6206.

Table 3. Factor Analysis of the KIEs

reaction	η_{trans}	η_{rot}	η_{low}[a]	η_{mid}	η_{high}[b]
$F^-(D_2O) + CH_3Cl$	1.05	1.35	0.74	1.14	0.55
$F^-(H_2O) + CD_3Cl$	1.04	1.66	0.61	1.07	0.74
$F^-(D_2O) + CD_3Cl$	1.09	2.24	0.45	1.21	0.41

[a] Contribution from modes with $\nu_i < 600$ cm^{-1}. [b] Contribution from modes with $\nu_i > 2000$ cm^{-1} in perprotio case.

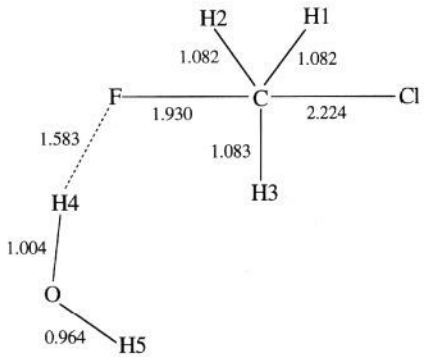

Figure 1. Transition state structure with bond lengths in Å given in the figure and bond angles ∠Cl–C–F = 179.1°, ∠Cl–C–H1 = 91.9°, ∠Cl–C–H2 = 91.6°, ∠Cl–C–H3 = 92.2°, ∠C–F–H4 = 109.9°, ∠F–H4–O = 175.6°, ∠H4–O–H5 = 102.5°. The dihedral angles along the backbone are –31.0° (H5–O–H4–F), –43.1° (O–H4–F–C), and 156.4° (H4–F–C–Cl).

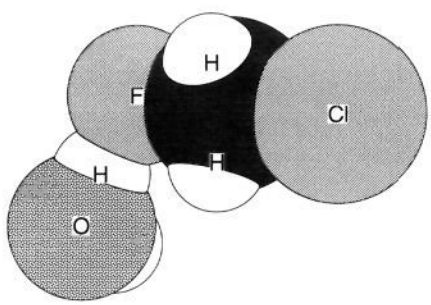

Figure 2. Space-filling view of the transition state structure.

One interesting point is that, within 0.2%, the KIE for $F^-(D_2O) + CD_3Cl$ is the product of those for $F^-(D_2O) + CH_3Cl$ and $F^-(H_2O) + CD_3Cl$. This agrees well with experiment.

Such excellent agreement of the calculated KIEs with experiment would seem to imply that the calculated transition state structure must be quantitatively valid and recrossing effects negligible (or surprisingly isotope-independent). The calculated transition state structure is illustrated in Figures 1 and 2. Of special interest is the bond angle at the hydrogen bond, 175.6°. The C–H stretch frequencies increase from 3105, 3225, and 3225 cm^{-1} in reactants to 3207, 3419, and 3426 cm^{-1} at the transition state. The most isotopically sensitive low-frequency modes are the second and third lowest-frequency modes (ν_{18} and ν_{19}) of the transition state. In particular, ν_{18} is most sensitive to D_2O substitution, changing from 96 to 79 cm^{-1}, and ν_{19} is most sensitive to CD_3 substitution, changing from 48 to 39 cm^{-1}. These modes are positive and negative linear combinations of the methyl group internal rotation and the bending motion of H5 (see labeling in Figure 1) out of the equilibrium plane of the water molecule. The highly inverse KIE contribution from the high-frequency modes in the D_2O substitution is from the stretching vibration between oxygen atom and the hydrogen atom that is hydrogen-bonded to the fluorine atom.

Traditional accounts[21,22] of solvent isotope effects (SIEs) have focused on several possible explanations for the observed results, with a major emphasis on (i) solvent structural stability (structure making and breaking) as manifested in solvent librational degrees of freedom (restricted rotations of solvent molecules due to solvent structure) and the stability of solvent hydrogen-bonded structures, and, to a lesser extent, on (ii) internal vibrations, especially O–H and O–D stretches, of solvent molecules perturbed by hydrogen bonding to the solute. The former effect was originally treated by Swain and Bader[23] and the latter by Bigeleisen[24] and Bunton and Shiner.[25] A continuing difficulty in interpretation of SIEs has been the lack of firm experimental basis for distinguishing these effects.[21-28] The new experimental results of Bierbaum and co-workers on microsolvation isotope effects provide an important contribution to filling that gap.

Laughton and Robertson,[22] in one example of the traditional analysis, attributed observed kinetic solvent isotope effects (KSIEs) largely to solvent reorganization around the anion; in particular, recognizing that there is a different charge distribution for reactant and transition state structures, they attributed the KSIE to "the difference in the energy required to break down the respective solvent structures in H_2O and D_2O contiguous to the halide". They especially emphasized the entropy change in S_N2 mechanisms, an experimental observable that they emphasized as a way to differentiate librational effects (which have a significant entropic contribution) from internal-solvent vibrational effects (which do not). Bigeleisen,[24] Bunton and Shiner,[25] and Newton and Friedman[29] discussed thermodynamic and kinetic solvent isotope effects in terms of the weakening of O–H (or O–D) bonds in first-hydration-shell coordinated water molecules. It is interesting to re-examine the present results for microsolvent KIEs (μKIEs) in light of the traditional approaches to bulk SIEs and bulk KSIEs.

Table 3 shows that the μKIEs are dominated by the high-frequency modes, and on further examination this contribution is indeed mostly due to the O–H and O–D stretching modes, the effect singled out earlier by Bigelsisen, Bunton and Shiner, and Newton and Friedman. The low-frequency modes associated with microsolvent librations also contribute but to a quantitatively lesser extent.

Finally we dissect the high-frequency contribution in more detail. The stretching frequencies of isolated H_2O are about 3935 and 3834 cm^{-1}. In $F^-(H_2O)$, we calculated 3878 cm^{-1} for the spectator O–H mode and 2261 cm^{-1} for the hydrogen-bonded O–H mode. In proceeding to the transition state the $F^-\cdots H_2O$ hydrogen bond is still completely formed (in particular there is no bridging to the Cl^- and no contribution from $Cl^-\cdots H_2O$), but the hydrogen bond is weaker. The reason for this is incipient charge delocalization from $F^-(H_2O)$ onto Cl. We calculated the partial charge on F^- by ChelpG analysis[30] of the MP2 density and found it decreases from 0.89 to 0.71 as one proceeds from $F^-(H_2O)$ to the transition state. [Although the MP2 ChelpG partial charges are considered to be our most reliable values, similar *trends* (but different magnitudes) are obtained at lower levels (see Table 4), including Hartree–Fock (HF) wave functions at the MP2 geometries or use of Mulliken analysis[31] or the original[32] Chelp procedure to extract partial charges. However, use of the Hartree–Fock method to optimize the geometries, followed by Mulliken analysis of the HF wave functions, is inadequate, yielding a partial charge of 0.97 for both reactant

(21) Arnett, E. M.; McKelvey, D. R. In *Solute–Solvent Interactions*; Coetzee, J. F., Ritchie, C. D., Eds.; Marcel Dekker: New York, 1969; p 343.
(22) Laughton, P. M.; Robertson, R. E. In *Solute–Solvent Interactions*; Coetzee, J. F., Ritchie, C. D., Eds.; Marcel Dekker: New York, 1969; p 399.
(23) Swain, C. G.; Bader, R. F. W. *Tetrahedron* **1960**, *10*, 182.
(24) Bigeleisen, J. *J. Chem. Phys.* **1960**, *32*, 1583.
(25) Bunton, C. A.; Shiner, V. J., Jr. *J. Am. Chem. Soc.* **1961**, *83*, 3207.
(26) Swain, C. G.; Thornton, E. R. *J. Am. Chem. Soc.* **1962**, *84*, 822.
(27) Robertson, R. E. *Prog. Phys. Org. Chem.* **1967**, *4*, 213.
(28) Thornton, E. K.; Thornton, E. R. In *Isotope Effects in Chemical Reactions*; (ACS Monograph 167), Van Nostrand Reinhold: New York, 1970; p 213.
(29) Newton, M. D.; Friedman, H. L. *J. Chem. Phys.* **1985**, *83*, 5210.
(30) Breneman, C. M.; Wiberg, K. B. *J. Comput. Chem.* **1990**, *11*, 361.
(31) Mulliken, R. S. *J. Chem. Phys.* **1955**, *23*, 1833.
(32) Chirlian, L. E.; Francl, M. M. *J. Comput. Chem.* **1987**, *8*, 894.

Table 4. Calculated Partial Charges on the Fluorine Atom with the aug-cc-pVDZ Basis Set

	HF Mulliken	MP2 Mulliken	MP2 Chelp	MP2 ChelpG
reactant[a]	−0.91	−0.91	−0.84	−0.89
transition state[a]	−0.89	−0.77	−0.72	−0.71

[a] At geometry calculated by MP2 level of theory.

and transition state.] As a consequence of the decreased fluorine partial charge at the transition state, the F⁻···H distance increases from 1.41 to 1.58 Å, and the O–H stretching frequency increases from 2261 to 3124 cm^{-1}, about 863 cm^{-1} closer to the unperturbed O–H stretching frequency. This change is accompanied by a decrease in the O–H bond length from 1.06 to 1.00 Å. The spectator O–H frequency continues to be largely unperturbed, with its frequency changing from 3878 to 3889 cm^{-1} as one proceeds from reactant to transition state and its bond distance remaining at 0.96 Å. Thus the H_2O molecule looks more like isolated water when it solvates the transition state than when it solvates reactants.

When H_2O is replaced by D_2O, the critical O–D frequencies associated with the hydrogen bond are 1656 in $F^-(D_2O)$ and 2274 cm^{-1} at the transition state. (The increase, 618 cm^{-1}, is 245 cm^{-1} less than that in the H_2O case.) Since the isotopically sensitive, reaction-coordinate-sensitive frequency increases as the reaction progresses to the transition state, the μSKIE is inverse. (Normal KIEs are associated with isotopically sensitive frequencies that decrease on proceeding to the transition state.)

Acknowledgment. The authors are grateful to Veronica Bierbaum for a preprint of ref 5 and for several helpful discussions. Encouragement to work on this problem from both Dr. Bierbaum and Chuck DePuy is also gratefully acknowledged. This work was supported in part by the U.S. Department of Energy, Office of Basic Energy Sciences.

Supplementary Material Available: Tables of geometries, absolute energies, and vibrational frequencies for all stationary points (7 pages). This material is contained in many libraries on microfiche, immediately follows this article in the microfilm version of the journal, and can be ordered from the ACS; see any current masthead page for ordering information.